

## SURFACE EXPLORATION AND PETROLOGICAL APPLICATIONS IN HIGH ENTHALPY GEOTHERMAL AREAS: A MULTIDISCIPLINARY APPROACH FOR THE CERRO PABELLÓN PROJECT (NORTHERN CHILE)

MARCO TAUSSI

Dipartimento di Scienze Pure e Applicate, Università di Urbino “Carlo Bo”, Via Ca’ le Suore 2/4, 61029 Urbino

### INTRODUCTION

The Cerro Pabellón geothermal system, located in the Pampa Apacheta of northern Chile (Fig. 1), is classified as a hidden (or blind) high-enthalpy geothermal field ( $T > 200$  °C). In fact, the only hydrothermal manifestations are represented by two fumaroles located on the top of the Apacheta volcano, westward and about 600 m higher than the Cerro Pabellón geothermal area, which is set at ~4,500 m a.s.l. (Fig. 1b). The area is part of the Altiplano-Puna Volcanic Complex (APVC; de Silva, 1989), an ignimbritic plateau between 21–24° South and straddling Chile, Bolivia and Argentina in the Andean Central Volcanic Zone (CVZ; Fig. 1).

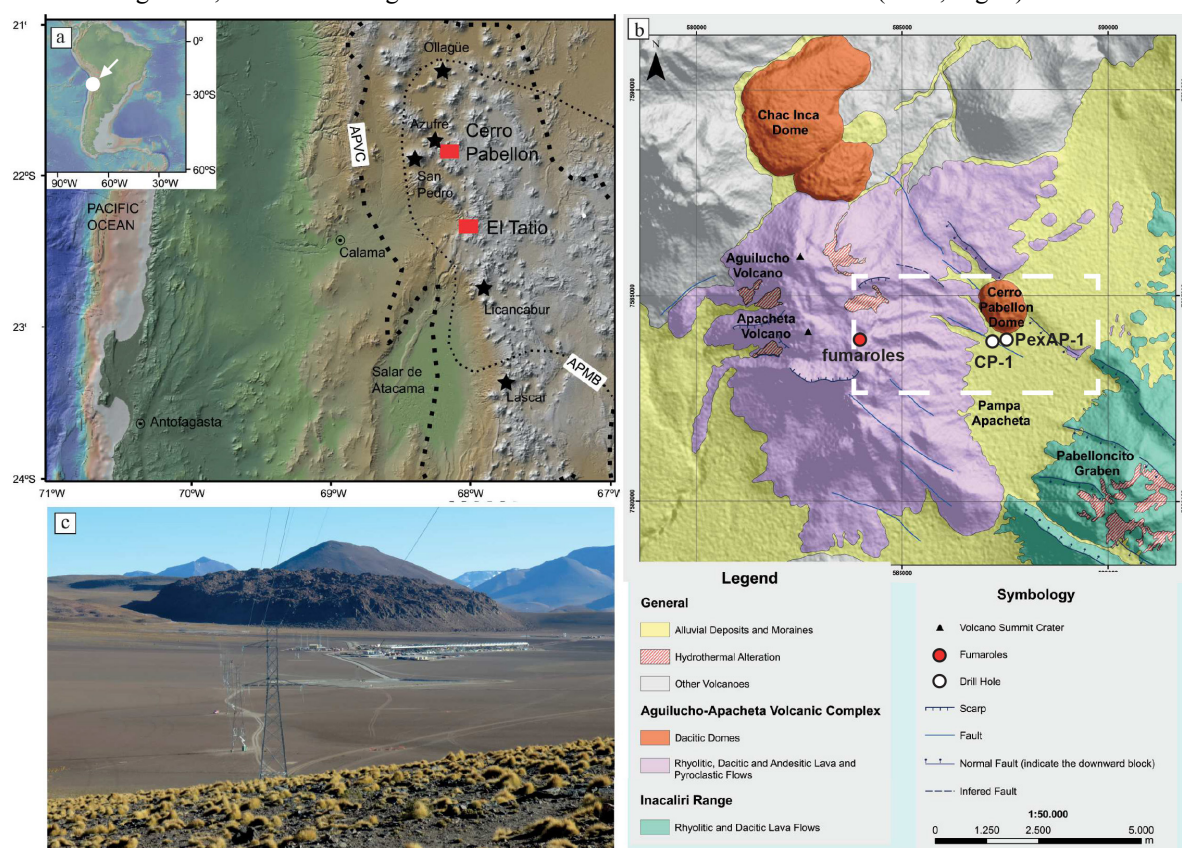


Fig. 1 - (a) CVZ of the Andes showing the APVC and the APMB surface projection, the main Pleistocene to Holocene volcanoes and the location of the Cerro Pabellón geothermal system; (b) simplified geological map of the studied area with indicated the boreholes studied, the area investigated through soil CO<sub>2</sub> and temperature measurements (white dashed rectangle) and the AAVC fumaroles; (c) general view of the Cerro Pabellón geothermal power plant. Modified from Maza *et al.* (2018).

The overthickened crust (up to 70 km) below the APVC hosts a partially-molten amalgamated igneous body called the Altiplano-Puna Magma Body (APMB; Chmielowski *et al.*, 1999). This magmatic body has been well constrained by seismic (Ward *et al.*, 2014), gravimetric (del Potro *et al.*, 2013) and magnetotelluric studies (Comeau *et al.*, 2015), and is interpreted as a batholith (Kern *et al.*, 2016) corresponding to a zone of melting,

assimilation, storage and homogenization (MASH, Hildreth & Moorbath, 1988) at upper crustal levels (*i.e.*, 10–25 km depth). This igneous body represents a “mush” column which contaminates the mantle-derived magmas with different degrees of assimilation (*e.g.*, Godoy *et al.*, 2017).

The aim of this PhD research project was to: *i)* deepen the knowledge concerning the heat source and the evolution of the related magmatic plumbing system, *ii)* define the clay-cap units, and *iii)* constrain their role in preventing the circulation of fluids toward the surface. A multidisciplinary approach was thus involved and focused on three complementary studies: *1)* A petrological, geochemical and isotopic study of the extrusives of the Apacheta-Aguilucho Volcanic Complex (AAVC) and of the most recent volcanic products of the APVC, represented by the dacitic domes of Chanka, Chac-Inca and Pabellón and the andesitic enclaves therein. *2)* A mineralogical study, by means of X-Ray Powder Diffraction (XRD) analysis, of samples from a production geothermal well and an exploration drill core, in order to examine the vertical distribution of the clay minerals forming the hydrothermal system of the Cerro Pabellón active geothermal field and define the clay-cap units of the system. *3)* A geochemical study of the diffuse soil CO<sub>2</sub> flux and temperature measurements in the Pampa Apacheta, coupled with soil temperature gradients carried out at the fumarolic field, in order to define the effectiveness of the clay-cap units and their importance in preventing the rise of the fluids toward the surface.

The final goal was to give a multidisciplinary conceptual model of a hidden geothermal system, combining geological, volcanological, mineralogical, petrological and geochemical investigations. The presence of the first geothermal power plant operating in South America was a great opportunity to study and deepen the main features of the Cerro Pabellón system. A major understanding of the processes involved in the formation of hidden geothermal areas is a challenge to extend exploration to other feasible zones where no surface manifestations are recognized.

## THE AAVC MAGMATIC PLUMBING SYSTEM

The evolution in the last 1 Ma of the magma plumbing system of the Pleistocene AAVC area (northern Chile) was investigated through petrographic, geochemical and isotopic studies of representative lavas.

Lavas from the AAVC, domes and related enclaves, pertain to the high-K calc-alkaline series and display a broad range in SiO<sub>2</sub> content (from 57.7 to 69.6 wt.%). Almost all the studied samples (lavas, domes and enclaves) form uniform trends in most of the bivariate diagrams between SiO<sub>2</sub> and the other major elements (Taussi *et al.*, 2019a). From amphibole thermobarometry applied on samples of the domes (both dacite and enclaves) and AAVC lavas, a low-pressure evolution and two distinct crystallization zones were recognized (Gorini *et al.*, 2018). The two distinct areas located at 15–20 km and at 4–8 km were interpreted as two different crustal level of magma storage. The deepest one is related to the APMB, whereas the shallowest one to the magmatic chambers of the AAVC and the domes (Fig. 2a). This is in agreement with the trace element ratios reported in Fig. 2 characterized by low Sr/Y (< 45; Fig. 2b) and low Sm/Yb (< 3.8; Fig. 2c) that can exclude a “thick crust assimilation” garnet signature (Mamani *et al.*, 2010). The APMB played a significant role in the magmatic plumbing systems of the erupted magmas at the AAVC and more generally at the APVC. Rising parental magma interacted with this voluminous magmatic body, resulting in strong contamination (Godoy *et al.*, 2017). In fact, the andesitic magmas (enclaves) were affected by processes of Assimilation plus Fractional Crystallization (AFC) during their ascent through the upper crust, presumably by the interaction with the APMB (15–20 km). These andesitic magmas were erupted with no or minor additional contamination at shallower levels, or experienced plagioclase-dominated Fractional Crystallization (FC) to dacite within shallower crustal magma chambers (4–8 km depth; Fig. 3). The constructional phase of the Apacheta and Aguilucho stratovolcanoes (~1 to ~0.6 Ma; Sellés & Gardeweg, 2017) reflect a transition from high flux to steady state magmatism, as also documented in other Pleistocene volcanic complexes of the APVC (Burns *et al.*, 2015). During this latter stage the mafic magma recharge was high enough to permit a large spectrum of hybridization of the resident magmas in the upper crust to form the abundant andesites and dacites lavas erupted at the AAVC. At ~150 ka, the magmatism turned to a new stage of recharge with episodic intrusion of small-volumes of

andesitic magmas (Godoy *et al.*, 2019) permitting the remobilization of the crystal-rich dacites, triggering the extrusions of the Chanka, Chac-Inca and Pabellón domes (Taussi *et al.*, 2019a).

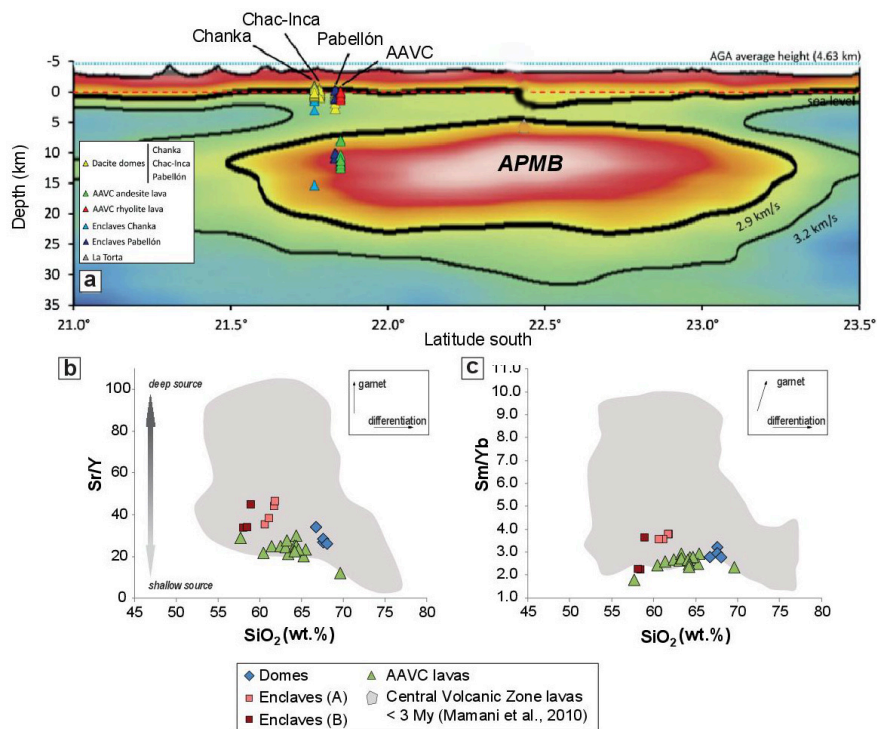


Fig. 2 - a) Seismic tomography cross-section of APMB reporting the crystallization depth of amphiboles (referred to sea level; red dashed line); modified from Gorini *et al.*, 2018; b) Plots of Sr/Y and c) Sm/Yb ratios versus SiO<sub>2</sub> for the studied samples; modified from Taussi *et al.* (2019a).

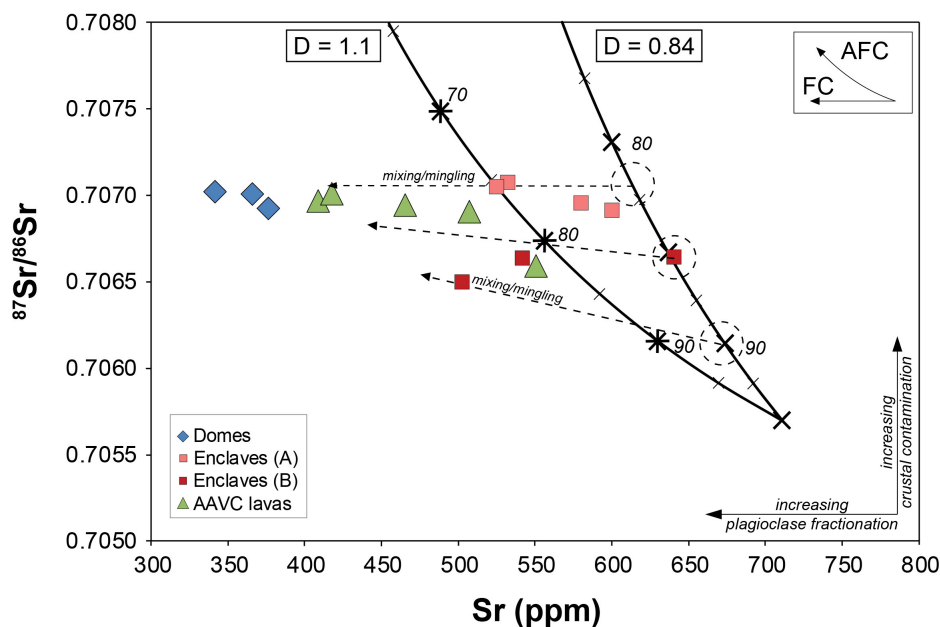


Fig. 3 - <sup>87</sup>Sr/<sup>86</sup>Sr vs. Sr (ppm) diagram showing the isotopic distribution of lavas from the AAVC sector. Black, bold lines represent plagioclase-dominated AFC-type (DePaolo, 1981). For details on the contaminant and initial endmembers see Taussi *et al.* (2019a). Italic numbers indicate the remaining melt fraction. The enclaves follow AFC trends, involving mixing/mingling processes (dashed lines) starting from different possible batches of less-differentiated magmas toward the dacitic domes samples. The AAVC samples follow a linear trend similar to FC plus mixing paths. Modified from Taussi *et al.* (2019a).



Similar mineral assemblages were recognized along both wells. Smectite is the main clay mineral in the ~165-250 m interval which is also characterized by the absence of quartz and the presence of clinoptilolite, calcite, alunite, pyrite and hematite. From ~250 to ~500 m, mixed-layer illite-smectite and chlorite-smectite linked to albite, calcite, hematite, quartz, stilbite and laumontite were identified. At about 375 m starts to appear corrensite, which is found in different samples until 575 meters. From ~400 m smectite group minerals rapidly decrease, while chlorite is intimately associated with hematite, adularia, albite, calcite, quartz, epidote. Illite was identified from ~500 m. The Ca-zeolites (clinoptilolite-stilbite-laumontite-wairakite sequence) are present from 165 m in a relatively discontinuous way. From ~500 m, it is possible to recognize epidote, sporadically at first and then in a persistent way from 625 m.

Various mineral assemblages down the boreholes were recognized and interpreted in terms of hydrothermal alteration facies. The shallower part can be referred to an argillic alteration facies. This zone is characterized by the occurrence of clinoptilolite and smectite as index minerals and temperatures between 90 °C and 175 °C (175-315 m depth). The sub-propylitic zone (315-490 m depth) is characterized by the replacement of smectite for illite-smectite mixed layers, whose amount decreases with increasing depth and temperature. This decrease is accompanied by the appearance of chlorite and laumontite, which take place at 180-185 °C. The argillic and sub-propylitic zones represent the clay-cap units, characterized by low permeability, temperatures <190 °C and about 300 m of thickness. Finally, the propylitic zone, with the chlorite-epidote-illite association (from about 500 m downwards) and temperatures >200 °C, likely represents the begin of the reservoir domain. From the mineralogical assemblages and relative facies, the geothermal reservoir seems to be characterized by an adularia-sericite alteration types, likely associated with neutral pH fluids (Heald *et al.*, 1987).

#### SEALING CAPACITY OF CLAY-CAP UNITS OF THE GEOTHERMAL RESERVOIR

An integrated methodology of soil CO<sub>2</sub> flux and temperature measurements was applied with the purpose of shedding light on the processes that have masked any hydrothermal surface features in the hidden geothermal system of Cerro Pabellón. CO<sub>2</sub> soil flux and temperatures using the accumulation chamber method (Chiodini *et al.*, 1998), on a grid of ~430 points, were measured in: *i*) the eastern flank of AAVC, *ii*) the western sector of Pampa Apacheta, and *iii*) the northernmost lineament bounding the Pabelloncito graben (Fig. 1b). Moreover, soil temperature gradient measurements were carried at the AAVC fumarolic field on the top of the Apacheta volcano at ~5,150 m a.s.l.

Based on the graphical statistical method (GSA) of the CO<sub>2</sub> flux values, two different populations (A and B) were recognized, possibly related to different sources and/or geochemical processes. Measured values of the CO<sub>2</sub> flux varied between 0.0 and 2.98 gm<sup>-2</sup>day<sup>-1</sup> (mean = 0.68 gm<sup>-2</sup>day<sup>-1</sup>), with the associated soil temperatures ranging between 7.6 °C and 29.8 °C (mean = 19.4 °C). However, no spatial correlation has been obtained between these data. The low values of population A (*i.e.*, <1.35 gm<sup>-2</sup>day<sup>-1</sup>) have been related to CO<sub>2</sub> fluxes associated with biologic activity, that can be considered as “background” threshold for the studied area (Taussi *et al.*, 2019b), since a homogeneous soil coverage with a vegetation mainly represented by small scattered shrubs and grass. Thus, population B (ranging between 1.35 and 2.98 gm<sup>-2</sup>day<sup>-1</sup>) should reflect increasing gas emissions from an endogenous, or at least a mixed endogenous-biogenic source. However, the CO<sub>2</sub> emission rates, and the mean output calculated at Cerro Pabellón, reflect a negligible degassing also from the geothermal system, when compared with those of volcanic systems from the Andes or other geothermal areas worldwide (Taussi *et al.*, 2019b).

Unlike the CO<sub>2</sub> flux values, soil temperatures show a different statistical behaviour. From the GSA method, only one population of values was recognized. Most temperature data exceeded ~10°C, that was considered a “background” threshold (Taussi *et al.*, 2019b). Being the soil temperature only partially modulated by ambient temperature in most of the sampling sites (R<sup>2</sup> = 0.53), these relatively high values seem to be associated to an endogenous process. Water boiling temperature at about 4,500 m a.s.l. (~88 °C) was reached at the bottom of well PAE-1, located in the eastern margin of the geothermal system (*i.e.*, near PexAP-1; Fig. 1b)

and above the clay-cap units identified through XRD analysis. The condensate sample from this well is meteoric in origin and significantly depleted in  $^{18}\text{O}$  and  $^2\text{H}$  (Urzua *et al.*, 2002), suggesting multiple boiling and condensation processes at shallow depths.

Thus, the high temperature reached at PAE-1, as well as the extensive weak thermal anomaly recognized at the surface, can be attributed to the existence of a shallow aquifer(s) heated by geothermal fluids. This could explain the thermal character of the aquifer(s), into which acidic compounds may dissolve, as shown by the low concentrations of  $\text{H}_2\text{S}$  measured in the PAE-1 gas samples (Urzua *et al.*, 2002). Conversely, the strong  $\text{CO}_2$  flux characterizing the fluids at the fumarolic field, where the largest heat and mass transfer occurs, prevented the complete dissolution of the highly soluble magmatic gases in the shallow groundwater. Here  $\text{SO}_2$  and  $\text{HCl}$  were detected in considerable amounts (Tassi *et al.*, 2010), while they were not recorded in well PAE-1. As a matter of fact, the only significant thermal anomaly was registered at the active AAVC fumarolic field, where temperatures of  $\sim 83^\circ\text{C}$  and temperature gradients up to  $\sim 2^\circ\text{C}/\text{cm}$  were registered.

## CONCLUSIONS

A polybaric upper crustal magma plumbing system has been working during the  $\sim 1$  Ma span time of activity of the AAVC area, with two distinct reservoirs (Fig. 2). The deeper one was located at mid-crustal levels (15-20 km) akin to the location given for the APMB, involving AFC processes with a dominant role played by amphibole fractionation. Shallower magma chambers located at depth of 4-8 km allowed further differentiation of the erupted magmas through FC processes, mainly dominated by plagioclase crystallization.

As a matter of fact, some uncertainties remain on the origin of the main heat source. According to numerical studies of Garcia-Estrada *et al.* (2002), high temperatures ( $\sim 300^\circ\text{C}$ ) in hydrothermal systems can only exist if the magmatic heat source is less than  $\sim 0.4$  Ma (for rhyolitic intrusions at 4 km of depth). The absence of dated products between 0.6 - 0.1 Ma in the studied area do not allow to define a univocal, main heat source. Neither the petrological history of the dacitic domes, permitted to constrain their magma chamber as the main thermal engine of the Cerro Pabellón geothermal system. What is undoubted is that the presence of the huge APMB in the upper crust is not negligible and cannot be ruled out as a fundamental heat source of this and other geothermal systems of the APVC.

However, the magmatic fluids released from the heat source(s) during their rise to the surface, started to interact with the host rocks, producing mineralogical, textural and chemical variations of these latter, as a response to the thermal and chemical changes. Mineralogical studies on the vertical distribution of the clay minerals forming the active hydrothermal system of the Cerro Pabellón geothermal field, revealed that the system is characterized by an adularia-sericite alteration type. The shallow part of the system is represented by argillic and sub-propylitic zone, representing the thick clay-cap of the system, whereas the lower part is characterized by a propylitic alteration, likely linked to fluids with near-neutral pH derived by the magmatic gas scrubbing processes in the geothermal reservoir (Tassi *et al.*, 2010; Fig. 5).

The sealing capacity of these clay-cap units was then investigated through systematic diffuse soil  $\text{CO}_2$  flux and temperature measurements. The low  $\text{CO}_2$  flux, even above the existing pressurized reservoir, and the relatively large areas of thermal anomalies suggest the efficiency of the thick clay-cap to prevent the resurgence of fluids up to the surface and the thermal behaviour of the aquifer(s) revealed by the slight and diffused thermal anomaly and the wispy flow of steam with measured temperature of  $88^\circ\text{C}$  at the bottom of the 187 m depth PAE-1 well (Fig. 5).

Finally, the decoupling between soil temperature and  $\text{CO}_2$  flux, defined that the volcano-tectonic structures did not play a key role in the distribution of the  $\text{CO}_2$  flux and temperature at surface, with the active fumarolic area representing the only visible evidence of the hidden geothermal reservoir. These results led to the update of the conceptual model of the Cerro Pabellón geothermal system, which was originally only composed by iso-resistivity and isotherm lines inferred from the MT survey of Urzua *et al.* (2002) (Fig. 5).

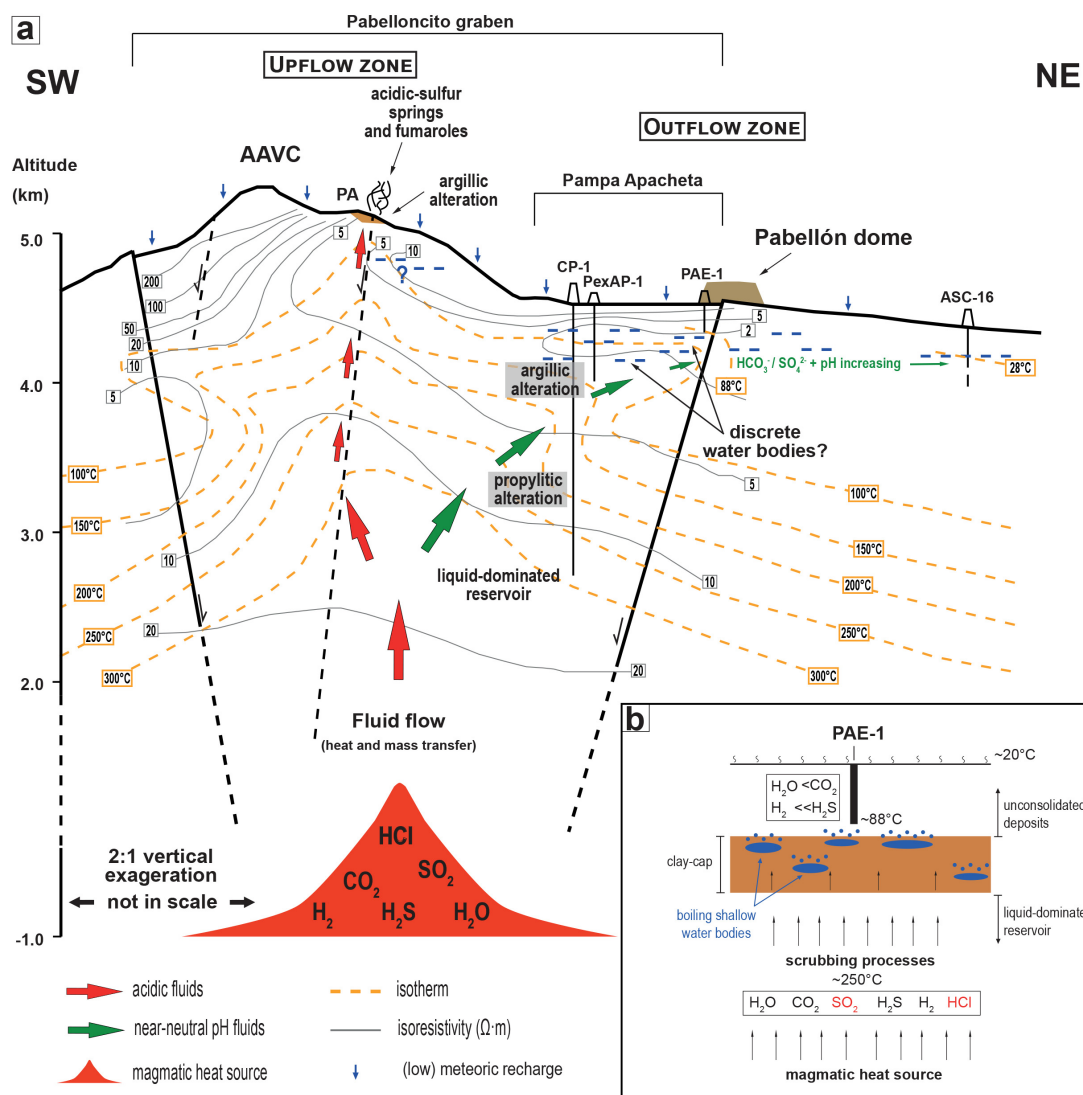


Fig. 5 - Conceptual model of the Cerro Pabellón geothermal field. a) simplified SW to NE profile of the Cerro Pabellón area showing temperature isotherms and resistivity data from Urzua *et al.* (2002). The fluids ascend from the magmatic heat source and follow two pathways: *i*) a direct ascent to the fumarolic field (acid fluids; upflow zone), or *ii*) the interaction with the liquid-dominated reservoir producing a  $\text{HCO}_3^-/\text{SO}_4^{2-}$  ratio and pH increase in the outflow zone. b) Schematic evolution of ascending geothermal fluids. Scrubbing processes characterized the reservoir, resulting in a lack of magmatic compounds at Pampa Apacheta; the  $\text{CO}_2$ -depleted steam rose, interacting with the shallower water bodies producing boiling; modified from Taussi *et al.* (2019b).

## REFERENCES

- Burns, D.H., de Silva, S.L., Tepley III, F., Schmitt, A.K., Loewen, M.W. (2015): Recording the transition from flare-up to steady-state arc magmatism at the Purico-Chascon volcanic complex, northern Chile. *Earth Planet. Sc. Lett.*, **422**, 75-86.
- Chiodini, G., Cioni, R., Guidi, M., Raco, B., Marini, L. (1998): Soil  $\text{CO}_2$  flux measurements in volcanic and geothermal areas. *Appl. Geochem.*, **13** (5), 543-552.
- Chmielowski, J., Zandt, G., Haberland, C. (1999): The Central Andean Altiplano-Puna magma body. *Geophys. Res. Lett.*, **26**, 783-786.
- Comeau, M.J., Unsworth, M.J., Ticona, F., Sunagua, M. (2015): Magnetotelluric images of magma distribution beneath Volcán Uturuncu, Bolivia: Implications for magma dynamics. *Geology*, **43**, 243-246.
- de Silva, S.L. (1989): Altiplano-Puna volcanic complex of the central Andes. *Geology*, **17** (12), 1102-1106.

- del Potro, R., Díez, M., Blundy, J., Camacho, A.G., Gottsmann, J. (2013): Diapiric ascent of silicic magma beneath the Bolivian Altiplano. *Geophys. Res. Lett.*, **40**, 2044-2048.
- DePaolo, D.J. (1981): Trace element and isotopic effects of combined wallrock assimilation and fractional crystallization. *Earth Planet. Sc. Lett.*, **53** (2), 189-202.
- García-Estrada, G.H., López-Hernández, A., Prol, L.R.M. (2002): Conductive thermal modeling to estimate the age of the heat source at the Los Azufres field, Mexico. *Geoth. Res. T.*, **26**, 22–25.
- Godoy, B., Wörner, G., Le Roux, P., de Silva, S., Parada, M.A., Kojima, S., González-Maurel, O., Morata, D., Polanco, E., Martínez, P. (2017): Sr- and Nd isotope variations along the Pleistocene San Pedro-Linzor volcanic chain, N. Chile: Tracking the influence of the upper crustal Altiplano-Puna Magma Body. *J. Volcanol. Geoth. Res.*, **341**, 172-186.
- Godoy, B., Taussi, M., González-Maurel, O., Renzulli, A., Hernández-Prat, L., Le Roux, P., Morata, D., Menzies, A. (2019): Linking the mafic volcanism with the magmatic stages during the last 1 Ma in the main volcanic arc of the Altiplano-Puna Volcanic Complex (Central Andes). *J. S. Am. Earth Sci.*, **95**, 102295.
- Gorini, A., Ridolfi, F., Piscaglia, F., Taussi, M., Renzulli, A. (2018): Application and reliability of calcic amphibole thermobarometry as inferred from calc-alkaline products of active geothermal areas in the Andes. *J. Volcanol. Geoth. Res.*, **358**, 58-76.
- Heald, P., Foley, N.K., Hayba, D.O. (1987): Comparative anatomy of volcanic-hosted epithermal deposits: acid-sulfate and adularia-sericite types. *Econ. Geol.*, **82** (1), 1-26.
- Hildreth, W. & Moorbath, S. (1988): Crustal contributions to arc magmatism in the Andes of Central Chile. *Contrib. Mineral. Petr.*, **98** (4), 455-489.
- Kern, J.M., de Silva, S.L., Schmitt, A.K., Kaiser, J.F., Iriarte, A.R., Economos, R. (2016): Geochronological imaging of an episodically constructed subvolcanic batholith: U-Pb in zircon chronochemistry of the Altiplano-Puna Volcanic Complex of the Central Andes. *Geosphere*, **12** (4), 1-24.
- Mamani, M., Wörner, G., Sempere, T. (2010): Geochemical variations in igneous rocks of the Central Andean orocline (13°S to 18°S): tracking crustal thickening and magma generation through time and space. *Geol. Soc. Am. Bull.*, **122** (1-2), 162-182.
- Maza, S.N., Collo, G., Morata, D., Lizana, C., Camus, E., Taussi, M., Renzulli, A., Mattioli, M., Godoy, B., Alvear, B., Pizarro, M., Ramírez, C., Rivera, G. (2018): Clay mineral associations in the clay cap from the Cerro Pabellón blind geothermal system, Andean Cordillera, Northern Chile. *Clay Miner.*, **54** (2), 117-141.
- Rivera, G., Morata, D., Ramírez, C. (2015): Evolución vulcanológica y tectónica del área del Cordón Volcánico Cerro del Azufre – Cerro Inacaliri y su relación con el sistema geotérmico de Pampa Apacheta, II Región de Antofagasta, Chile. *Actas XIV Congreso Geológico Chileno*, La Serena, Chile, 556-559.
- Sellés, D. & Gardeweg, M. (2017): Geología del área Ascotán-Cerro Inacaliri, Región de Antofagasta. *Servicio Nacional de Geología y Minería, Carta Geológica de Chile, Serie Geología Básica*, **190**, 1-73.
- Tassi, F., Aguilera, F., Darrah, T., Vaselli, O., Capaccioni, B., Poreda, R.J., Delgado Huertas, A. (2010): Fluid geochemistry of hydrothermal systems in the Arica-Parinacota, Tarapacá and Antofagasta regions (northern Chile). *J. Volcanol. Geoth. Res.*, **192**, 1-15.
- Taussi, M., Godoy, B., Piscaglia, F., Morata, D., Agostini, S., Le Roux, P., González-Maurel, O., Gallmeyer, G., Menzies, A., Renzulli, A. (2019a): The upper crustal magma plumbing system of the Pleistocene Apacheta-Aguilucho Volcanic Complex area (Altiplano-Puna, northern Chile) as inferred from the erupted lavas and their enclaves. *J. Volcanol. Geoth. Res.*, **373**, 179-198.
- Taussi, M., Nisi, B., Pizarro, M., Morata, D., Veloso, E.E., Volpi, G., Vaselli, O., Renzulli, A. (2019b): Sealing capacity of clay-cap units above the Cerro Pabellón hidden geothermal system (northern Chile) derived by soil CO<sub>2</sub> flux and temperature measurements. *J. Volcanol. Geoth. Res.*, **384**, 1-14.
- Urzua, L., Powell, T., Cumming, W.B., Dobson, P. (2002): Apacheta, a new geothermal prospect in northern Chile. *Geoth. Res. T.*, **26**, 65-69.
- Ward, K.M., Zandt, G., Beck, S.L., Christensen, D.H., McFarlin, H. (2014): Seismic imaging of the magmatic underpinnings beneath the Altiplano-Puna volcanic complex from the joint inversion of surface wave dispersion and receiver functions. *Earth Planet. Sc. Lett.*, **404**, 43-53.